SDTC-EKF Control of an Induction Motor Based Electric Vehicle

B. Tabbache[1,2], A. Kheloui[2], M.E.H. Benbouzid[1], N. Henini[3]

Abstract–*This paper presents the experimental implementation of sensorless direct torque control of an induction motor based electric vehicle. In this case, stator flux and rotational speed estimations are achieved using an extended Kalman filter. Experimental results on a test vehicle propelled by a 1-kW induction motor seem to indicate that the proposed scheme is a good candidate for an electric vehicle control.*

Keywords: *Sensorless Direct Torque Control (SDTC), Extented Kalman Filter (EKF), Electric Vehicle (EV), DSP TMS320LF2407.*

I. Introduction

Electric vehicles are set to improve the energy and environmental impact of an increasing road transport population by offering a more energy efficient and less polluting drive-train alternative to conventional internal combustion engine vehicles. The electric vehicle production is then expected to increase dramatically these years.

The electric propulsion system is the heart of an EV [1]. It consists of the motor drive, transmission device, and wheels. In fact, the motor drive, comprising the electric motor, power converter, and electronic controller, is the core of the EV propulsion system. The motor drive is configured to respond to a torque demand set by the driver. The maintenance-free and low-cost induction motors became a good attractive alternative to many developers. However, high-speed operation of induction machines is only possible with a penalty in size and weight. Three-phase squirrel cage-rotor induction motors are best suited to electric vehicle drive applications thanks to its well-known advantage of simple construction, reliability, ruggedness, and low cost [2].

Induction motors constitute a theoretically challenging control problem since the dynamical system is nonlinear, the electric rotor variables are not measurable, and the physical parameters are most often imprecisely known. In addition, unlike the traditional industrial setting, in which the induction motor operates mostly at steady-state, the EV applications require high performance control of electric motors to obtain fast transient responses and energy efficiency. Important characteristics of an EV motor include good drive control and fault-tolerance, as well as low noise with high efficiency. The control EVs induction motor has attracted much attention in the past five years; especially sensorless speed control [3-4].

Induction motor drives control techniques are well treated in the literature. The most popular is the so-called vector control technique that is now used for high impact automotive applications. In parallel, a number of studies have been developed to find out different control solutions to achieve better dynamic performances of the induction motor drive. Among these techniques, DTC appears to be very convenient for EV applications [3], [5-6].

DTC has the advantages of simplicity; it does not require speed or position encoders and uses voltage and current measurements only to estimate flux, torque. It also has a faster dynamic response since it does not require any current regulation, coordinates transformation and insensitivity to motor parameters except the stator winding resistance [6]. The input of the motor controller is the reference speed, which is directly applied by the driver on the EV pedal.

DTC implementation requires the knowledge of two control values that are the electromagnetic torque and the stator flux. In standard induction motor drives, the control values are not accessible via sensors. It is then necessary to estimate or observe them. Stator flux can be simply estimated by integrating of the stator ohmic voltage drop. However, the use of a pure integrator leads to instabilities due signal offsets, inaccuracy and noises [7]. A more elaborated solution consists in using deterministic type of state observers such as the Luenberger observer or stochastic ones such as Kalman filter. In general the Lunberger observer achieves good results. However, in case of strongly nonlinear systems such as the induction motor, it is proved to be limited especially at low speeds [4]. This is why stochastic observers such the Extended Kalman Filter are preferred to estimate the stator flux, the electromagnetic torque and also the induction motor speed [7-8].

This paper presents then the experimental implementation of sensorless DTC of an induction motor based EV where the stator flux and rotational speed estimations are achieved using an EKF.

II. The Electric Vehicle Model

2.1 Nomenclature

v = vehicle speed;
α = Grade angle;
P_v = Vehicle driving power;
F_w = Road load;
F_{ro} = Rolling resistance force;
F_{sf} = Stokes or viscous friction force;
F_{ad} = Aerodynamic drag force;
F_{cr} = Climbing and downgrade resistance force;
μ = Tire rolling resistance coefficient;
m = Vehicle mass;
g = Gravitational acceleration constant;
k_A = Stokes coefficient;
ξ = Air density;
C_w = Aerodynamic drag coefficient ($0.2 < C_w < 0.4$);
A_f = Vehicle frontal area;
v_0 = is the head-wind velocity;
F = Tractive force;
k_m = Rotational inertia coefficient ($1.08 < k_m < 1.1$);
a = Vehicle acceleration;
J = Total inertia (rotor and load);
ω_m = Motor mechanical speed;
T_B = Load torque accounting for friction and windage;
T_L = Load torque;
T_m = Motor torque;
i = Transmission ratio;
η_t = Transmission efficiency;
R = Wheel radius;
J_V = Shaft inertia moment;
J_W = Wheel inertia moment;
λ = Wheel slip.

2.2. Dynamics Analysis

Based on principles of vehicle mechanics and aerodynamics, one can assess both the driving power and energy necessary to ensure vehicle operation (Fig. 1) [5].

The road load consists of

$$F_w = F_{ro} + F_{sf} + F_{ad} + F_{cr} \quad (1)$$

The rolling resistance force F_{ro} is produced by the tire flattening at the roadway contact surface.

$$F_{ro} = \mu mg \cos\alpha \quad (2)$$

μ is nonlinearly dependent of the vehicle speed, tire pressure and type, and road surface characteristic ($0.015 < \mu < 0.3$). It increases with vehicle speed and also during vehicle turning maneuvers.

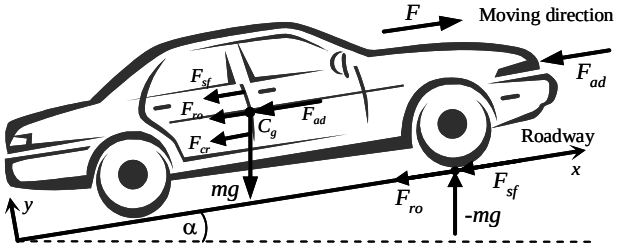

Fig. 1. Elementary forces acting on a vehicle.

The rolling resistance force can be minimized by keeping the tires as much inflated as possible.

$$F_{sf} = k_A v \quad (3)$$

Aerodynamic drag, F_{ad}, is the viscous resistance of air acting upon the vehicle.

$$F_{ad} = \frac{1}{2}\xi C_w A_f (v + v_0)^2 \quad (4)$$

The climbing resistance (F_{cr} with positive operational sign) and the downgrade force (F_{cr} with negative operational sign) is given by

$$F_{cr} = \pm mg \sin\alpha \quad (5)$$

The tractive force in an electric vehicle is supplied by the electric motor in overcoming the road load. The equation of motion is given by

$$k_m m \frac{dv}{dt} = F - F_w \quad (6)$$

The net force $(F - F_w)$, accelerates the vehicle (or decelerates when F_w exceeds F).

The power required to drive a vehicle has to compensate the road load F_w.

$$P_v = vF_w \quad (7)$$

The mechanical equation (in the motor referential) used to describe each wheel drive is expressed by

$$J \frac{d\omega_m}{dt} + T_B + T_L = T_m \quad (8)$$

The following equation is derived due to the use of a reduction gear.

$$\begin{cases} \omega_{Wheel} = \dfrac{\omega_m}{i} \\ T_{Wheel} = T_m i \eta_t \end{cases} \quad (9)$$

The load torque in the motor referential is given by.

$$T_L = \frac{T_{LWheel}}{i} = \frac{R}{i} F_\omega \qquad (10)$$

The vehicle global inertia moment in the motor referential is given by

$$\begin{cases} J = J_W + J_V \\ J_V = \frac{1}{2} m \frac{R^2}{i^2} (1 - \lambda) \end{cases} \qquad (11)$$

If the adhesion coefficient of the road surface is high, then λ is usually low and can be neglected.

III. Direct Torque Control

3.1 Nomenclature

s, (*r*)	=	Stator (rotor) index;
α, β	=	Synchronous reference frame index;
*	=	Reference;
est	=	Estimation index;
V (*i*)	=	Voltage (Current);
φ	=	Flux;
ω_r	=	Rotor electric speed;
T_{em}	=	Motor torque;
R	=	Resistance;
L	=	Inductance;
L_m	=	Magnetizing inductance;
σ	=	Leakage coefficient, $\sigma = 1 - L_m^2/L_sL_r$;
p	=	pole-pair number;
T	=	Sampling time.

3.2 The DTC Briefly

The basic idea of the method is to calculate flux and torque instantaneous values only from the stator variables [3], [9]. In this case, flux, torque, and speed are estimated, by and EKF in our case. The input of the motor controller is the reference speed, which is directly applied by the driver on the EV pedal. The control is carried out by hysteresis comparators and a switching logic table selecting the appropriate voltage inverter switching configurations [3], [5]. Figure 2 gives the global configuration of a DTC scheme and also shows how the EV dynamics will be taken into account (λ is also the flux).

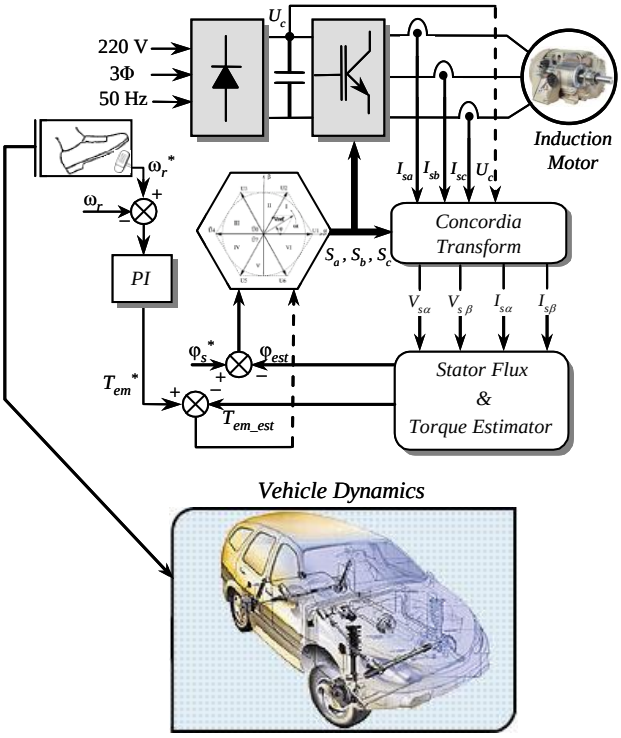

(a)

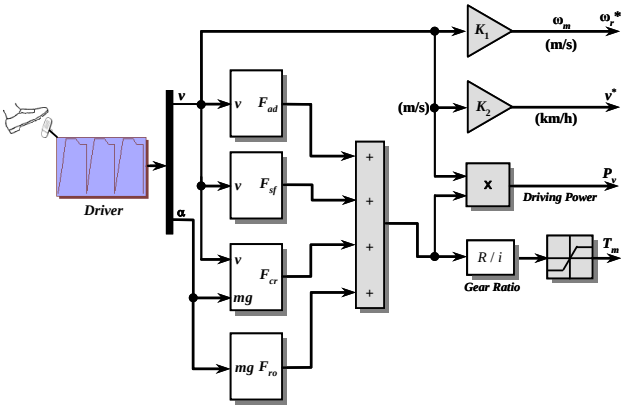

(b) EV dynamics.

Fig. 2. DTC general configuration.

III. Extended Kalman Filter

The Kalman filter, is a special class of linear observer (deterministic type), derived to meet a particular optimality stochastic condition. The Kalman filter has two forms: basic and extended. The EKF can be used for nonlinear systems. This means that the plant model is extended by extra variables, in our case by the mechanical speed [10].

In the induction motor drive, the Kalman filter is used to obtain unmeasured state variables (rotor speed ω_r, rotor flux vector components $\varphi_{\alpha r}$ and $\varphi_{\beta r}$) using the measured state variables (stator current and voltage components in Concordia frame α-β). Moreover, it takes into account the model and measurement noises [10-11].

The state model of the induction motor used by the Kalman filter is developed in the stationary reference frame and summarized by (7) [7].

The implementation of the Kalman filter is based on a recursive algorithm minimizing the error variance between the real variable and its estimate.

Let us consider a linear stochastic system whose discrete state model is given b y (8).

$$\begin{cases} \dfrac{d}{dt}\begin{bmatrix} i_{s\alpha} \\ i_{s\beta} \\ \varphi_{r\alpha} \\ \varphi_{r\beta} \\ \omega_r \end{bmatrix} = \begin{bmatrix} -\dfrac{K_R}{K_L} & 0 & \dfrac{L_m R_r}{L_r^2 K_L} & \dfrac{L_m \omega_r}{L_r K_L} & 0 \\ 0 & -\dfrac{K_R}{K_L} & \dfrac{L_m \omega_r}{L_r K_L} & \dfrac{L_m R_r}{L_r^2 K_L} & 0 \\ \dfrac{L_m}{T_r} & 0 & -\dfrac{1}{T_r} & -\omega_r & 0 \\ 0 & \dfrac{L_m}{T_r} & \omega_r & -\dfrac{1}{T_r} & 0 \\ 0 & 0 & 0 & 0 & 1 \end{bmatrix} \begin{bmatrix} i_{s\alpha} \\ i_{s\beta} \\ \varphi_{r\alpha} \\ \varphi_{r\beta} \\ \omega_r \end{bmatrix} + \dfrac{1}{K_L}\begin{bmatrix} 1 & 0 \\ 0 & 1 \\ 0 & 0 \\ 0 & 0 \\ 0 & 0 \end{bmatrix}\begin{bmatrix} V_{s\alpha} \\ V_{s\beta} \end{bmatrix} \\ \begin{bmatrix} i_{s\alpha} \\ i_{s\beta} \end{bmatrix} = \begin{bmatrix} 1 & 0 & 0 & 0 & 0 \\ 0 & 1 & 0 & 0 & 0 \end{bmatrix} \begin{bmatrix} i_{s\alpha} \\ i_{s\beta} \\ \varphi_{r\alpha} \\ \varphi_{r\beta} \\ \omega_r \end{bmatrix} \end{cases} \tag{7}$$

where $\dfrac{K_L}{K_R} = \left(\dfrac{R_s}{L_s} + \dfrac{1-\sigma}{\sigma T_r}\right)$ and $T_r = \dfrac{L_r}{R_r}$

$$\begin{cases} x(k+1) = Ax(k) + Bu(k) + w(k) \\ y(k+1) = Cx(k) + v \end{cases} \tag{8}$$

where $w(k)$ represents the disturbances vector applied to the system inputs. It also represents modeling uncertainties; $v(k)$ corresponds to system output measurement noises. It is supposed that the random signals $v(k)$ and $w(k)$ are Gaussian noises not correlated and with null average value. They are characterized by covariance matrixes, Q and R respectively, which are symmetrical and definite positive. The initial state vector x_0 is also a random variable with covariance matrix P_0 and average value $\bar{x}_0$.

The Kalman filter recursive algorithm could be summarized by the following steps (Fig. 3).

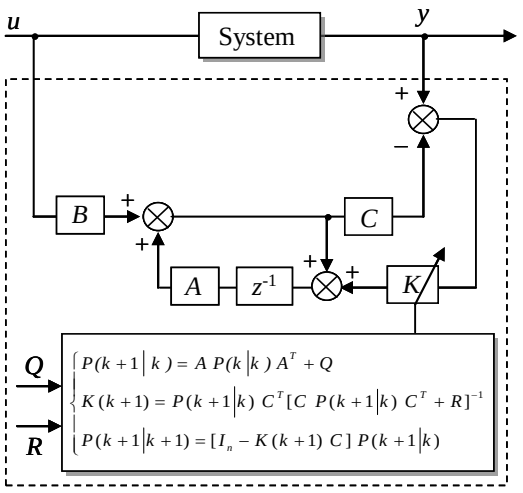

Fig. 3. The EKF algorithm.

– Initial State:

$$\hat{x}(0|0) = \bar{x}_0 \tag{9}$$

– State prediction:

$$\begin{cases} \hat{x}(k+1|k) = A\hat{x}(k|k) + Bu(k) \\ \hat{y}(k+1|k) = C\hat{x}(k+1|k) \end{cases} \tag{10}$$

– Error covariance matrix prediction:

$$P(k+1|k) = AP(k|k)A^T + Q \tag{11}$$

– Kalman gain:

$$K(k+1) = P(k+1|k)\,C^T[CP(k+1|k)\,C^T + R]^{-1} \tag{12}$$

– Filtering or correction of the predicted states:

$$\begin{aligned} \hat{x}(k+1|k+1) = {} & \hat{x}(k+1|k) \\ & + K(k+1)[y(k+1) - \hat{y}(k+1|k)] \end{aligned} \tag{13}$$

– Covariance matrix update:

$$P(k+1|k+1) = [I_n K(k+1)C]\,P(k+1|k) \tag{14}$$

For an induction motor, the Kalman filter must be used in its extended version. Therefore, a nonlinear stochastic system discrete state equation is given by:

$$\begin{cases} x_{k+1} = f(x_k, u_k) + w_k \\ y_k = h(x_k) + v_k \end{cases} \tag{15}$$

where f and h are vector functions.

$$f = \begin{bmatrix} \left(1 - T\frac{K_R}{K_L}\right) i_{s\alpha} + T\frac{L_m R_r}{L_r^2 K_L}\varphi_{r\alpha} + T\frac{L_m \omega_r}{L_r K_L}\varphi_{r\beta} + T\frac{1}{K_L}V_{s\alpha} \\ \left(1 - T\frac{K_R}{K_L}\right) i_{s\beta} - T\frac{L_m R_r}{L_r^2 K_L}\varphi_{r\alpha} + T\frac{L_m \omega_r}{L_r K_L}\varphi_{r\beta} + \frac{1}{K_L}V_{s\beta} \\ T\frac{L_m}{T_r} i_{s\alpha} + \left(1 - T\frac{1}{T_r}\right)\varphi_{r\alpha} - T\omega_r \varphi_{r\beta} \\ T\frac{L_m}{T_r} i_{s\beta} + T\omega_r \varphi_{r\alpha} + \left(1 - T\frac{1}{T_r}\right)\varphi_{r\beta} \\ \omega_r \end{bmatrix} \quad \text{and} \quad h = C_d x_{k|k+1} = \begin{bmatrix} i_{s\alpha} \\ i_{s\beta} \end{bmatrix}$$

The notation $k + 1$ is related to predicted values at $(k + 1)^{th}$ instant and is based on measurements up to k^{th} instant.

The EKF equations are similar to those of the linear Kalman filter with the difference that A and C matrixes should replaced by the Jacobians of the vector functions f and h at every sampling time as follows.

$$\begin{cases} A_k[i,j] = \left.\dfrac{\partial f_i}{\partial x_j}\right|_{x = \hat{x}(k|k)} \\ C_k[i,j] = \left.\dfrac{\partial h_i}{\partial x_j}\right|_{x = \hat{x}(k|k-1)} \end{cases} \tag{16}$$

The covariance matrixes R_k and Q_k are also defined at every sampling time.

For the induction motor control, the EKF is used for the speed real-time estimation. It can also be used to estimate states and parameters using the motor voltages and currents measurements.

IV. Experimental Implementation and Results

4.1 The Test Bench

The test bench used to validate the proposed control approach is made up of a 1-kW induction motor drive whose ratings are given in the Appendix. The main components of this bench, illustrated by Fig. 4, are:

- A DSP system (single fixed-point TMS320LF2407 DSP-based development board);
- An optical encoder attached to the motor shaft only to allow comparison between estimated and measured speed;
- Hall effect sensors for voltage and current measurements.

The DSP system is interfaced to a standard PC. The continuous-time algorithm is discredited with a sampling period of 100 µsec. At each sampling instant, the DSP receives stator current and voltage measurements and then runs the estimation algorithm and the DTC scheme.

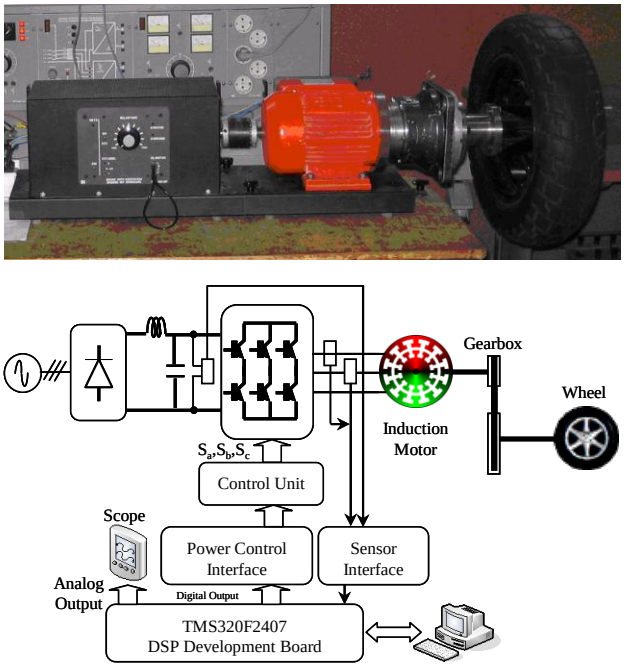

Fig. 4. The experimental setup.

It should be noted, as illustrated by Fig. 4, that the experimental setup was built to slightly emulate an EV. The EV resistance forces are emulated by a powder brake.

4.2 The Experimental Results

The estimation algorithm is tested under challenging load torque and speed variations. The experimentally obtained results are then summarized by Figs. 5 to 8.

In order to test the SDTC-EKF control scheme performances, the first experiments are carried out under a constant speed reference. Therefore, Fig. 5 to 7, respectively illustrating the stator currents, the flux, and the torque, prove the effectiveness of the proposed control scheme.

The proposed SDTC-EKF scheme has also been tested with a specific speed profile to assess its effectiveness for automotive applications (EV). In this case, Fig. 8 illustrates the sensorless control performances. It obviously proves the effectiveness of the proposed control scheme.

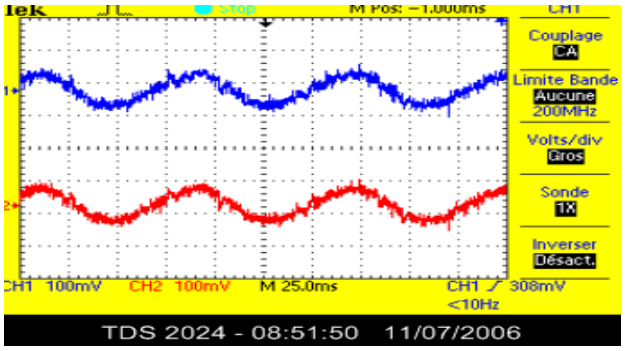

(a) i_α

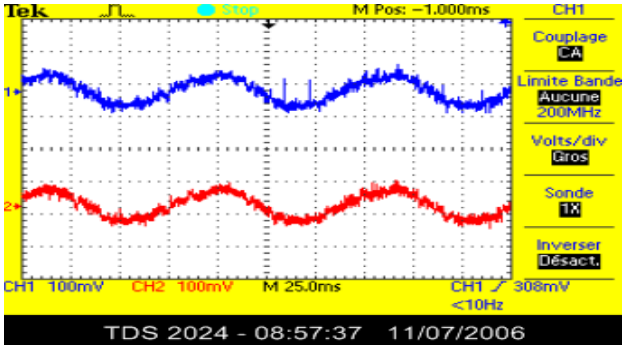

(b) i_β

Fig. 5. Stator current components:
Estimation (top/blue) and measurements (bottom/red).

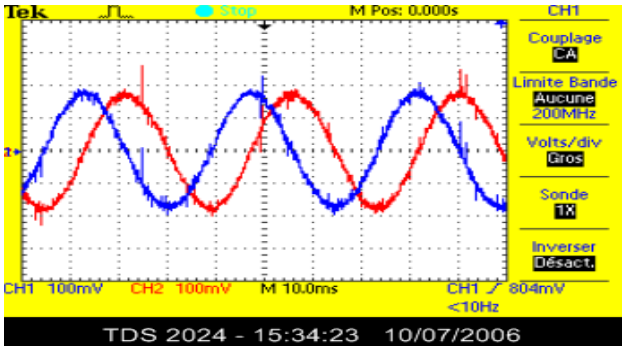

(a)

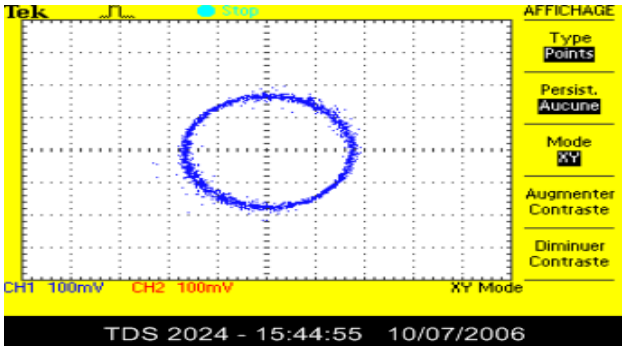

(b)

Fig. 6. Estimated (a) stator flux and flux trajectory (b).

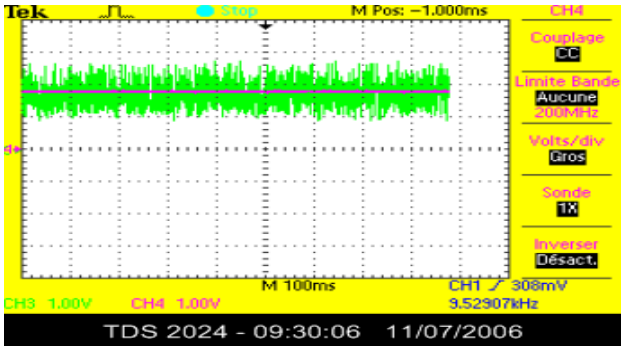

Fig. 7. The electromagnetic torque with a 2 Nm reference.

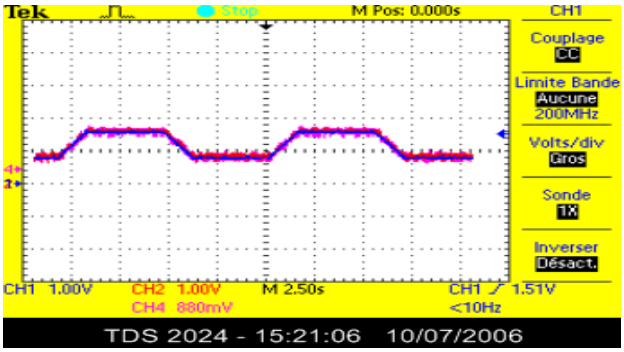

Fig. 8. Speed response to a trapezoidal speed profile
(measurements and estimation).

V. Conclusion

This paper has presented the experimental implementation of sensorless direct torque control of an induction motor based electric vehicle. In this case, stator flux and rotational speed estimations are achieved using an extended Kalman filter. Experimental results on a test vehicle propelled by a 1-kW induction motor prove the effectiveness of the proposed control scheme in terms of torque and speed performances.

The obtained results seem to indicate that SDTC-EKF scheme is a good candidate for the control of EVs induction motor based propulsion.

Appendix

Rated Data of the Tested Induction Motor

1 kW, 2.5 Nm, 2830 rpm, p = 1
R_s = 4.750 Ω, R_r = 8.000 Ω, L_s = 0.375 H, L_r = 0.375 H, M = 0.364 H
J = 0.003 kg.m², k_f = 0.0024 Nms

References

[1] C.C. Chan, “The state of the art of electric and hybrid vehicles,” *Proceedings of the IEEE*, vol. 90, n°2, pp. 247-275, February 2002.

[2] M.E.H. Benbouzid et *al.*, “Electric motor drive selection issues for HEV propulsion systems: A comparative study,” *IEEE Trans. Vehicular Technology*, vol. 55, n°6, pp. 1756-1764, November 2006.

[3] F. Khoucha et *al.*, "Electric vehicle induction motor DSVM-DTC with torque ripple minimization," *International Review of Electrical Engineering*, vol. 4, n°3, pp. 501-508, June 2009.

[4] A. Haddoun et *al.*, "Comparative analysis of estimation techniques of SFOC induction motor for electric vehicles," *in Proceedings of the ICEM'08*, Vilamoura (Portugal), September 2008.

[5] A. Haddoun et *al.*, "A loss-minimization DTC scheme for EV induction motors," *IEEE Trans. Vehicular Technology*, vol. 56, n°1, pp. 81-88, January 2007.

[6] G.S. Buja et *al.*, "Direct torque control of PWM Inverted-Fed AC Motors – A Survey," *IEEE Trans. Industrial Electronics*, vol. 51, n°4, pp. 744-757, August 2004.

[7] A. Bilal et *al.*, "Simple derivative-free nonlinear state observer for sensorless AC drives," *IEEE/ASME Trans. Mechatronics*, vol. 11, n°5, pp. 1083-4435, Octobre 2006.

[8] M. Barut et *al.*, "Experimental evaluation of braided EKF for sensorless control of induction motors," *IEEE Trans. Industrial Electronics*, vol. 55, n°5, pp. 620-632, February 2008.

[9] T. Brahmananda Reddy et *al.*, "Improvement of DTC performance by using hybrid space vector pulsewidth modulation algorithm," *International Review of Electrical Engineering*, vol. 2. n°1, pp. 593-600, August 2007.

[10] L. Harnefors, "Instability phenomena and remedies in sensorless indirect field oriented control," *IEEE Trans. Power Electronics*, vol. 15, n°4, pp. 733-743, July 2002.

[11] M. Bendjedia et *al.*, "Digital step motor drive with EKF estimation of speed and rotor position," *International Review of Electrical Engineering*, vol. 2. n°1, pp. 455-565, June 2007.

[1]University of Brest, EA 4325 LBMS, Rue de Kergoat, CS 93837, 29238 Brest Cedex 03, France (e-mail: Mohamed.Benbouzid@univ-brest.fr.
[2]Electrical Engineering Department, Polytechnic Military Academy, 16111 Algiers, Algeria.
[3]Electrical Engineering Department, Ecole National Supérieure Polytechnique, 10, Avenue Hassen Badi, BP 182, 16200 Algiers, Algeria.

Bekheira Tabbache was born in Chlef, Algeria in 1979. He received the B.Sc. and the M.Sc. degrees in electrical engineering, from the Polytechnic Military Academy, Algiers, Algeria, in 2003 and 2007 respectively. In 2004, he joined the Electrical Engineering Department of the Polytechnic Military Academy, Algiers, Algeria as a Teaching Assistant.

He is currently pursuing Ph.D. studies on electric vehicle fault-tolerant control.

Abdelaziz Kheloui received the M.Sc. degree in Electrical Engineering from the Ecole Nationale d'Ingénieurs et Techniciens of Algeria (ENITA), Algiers, Algeria in 1990 and the Ph.D. degree also in electrical engineering from the National Polytechnic Institute of Lorraine, Nancy, France in 1994. Since 1994 he has been an Assistant than an Associate Professor at the Electrical Engineering Department of the Polytechnic Military Academy, Algiers, Algeria.

His current research interests are control of electrical drives and power electronics.

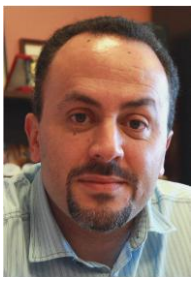

Mohamed El Hachemi Benbouzid was born in Batna, Algeria, in 1968. He received the B.Sc. degree in electrical engineering from the University of Batna, Batna, Algeria, in 1990, the M.Sc. and Ph.D. degrees in electrical and computer engineering from the National Polytechnic Institute of Grenoble, Grenoble, France, in 1991 and 1994, respectively, and the Habilitation à Diriger des Recherches degree from the University of Picardie "Jules Verne," Amiens, France, in 2000.

After receiving the Ph.D. degree, he joined the Professional Institute of Amiens, University of Picardie "Jules Verne," where he was an Associate Professor of electrical and computer engineering. In September 2004, he joined the University Institute of Technology (IUT) of Brest, University of Brest, Brest, France, as a Professor of Electrical Engineering. His main research interests and experience include analysis, design, and control of electric machines, variable-speed drives for traction and propulsion applications, and fault diagnosis of electric machines.

Noureddine Henini was born in Médéa, Algeria in 1976. He received the B.Sc. degree in electrical engineering from the University of Médéa, Médéa, Algeria, in 1998, and the M.Sc. degree in electrical engineering, from the Polytechnic Military Academy, Algiers, Algeria, in 2006.

He is currently pursuing Ph.D. studies on multiphase and multimachine systems.